Spring 5-9-2024

The Effects of UV Degradation on Polycarbonate Plastics Under Dynamic Compressive Loading

Hannah Bradford

THE EFFECTS OF UV-DEGRADATION ON POLYCARRBONATE PLASTICS UNDER DYNAMIC COMPRESSIVE LOADING

by
Hannah Hess Bradford

A thesis submitted to the faculty of The University of Mississippi in partial fulfillment of the requirements of the Sally McDonnell Barksdale Honors College.

Oxford
May 2024

Approved by

_____
Advisor: Dr. Damian Stoddard

_____
Reader: Dr. Arunachalam Rajendran

_____
Reader: Dr. Shan Jiang

ACKNOWLEDGEMENTS

The author would like to first and foremost thank her advisor Dr. Damian Stoddard for all his guidance, knowledge, and calm over the course of this project. Dr. Stoddard has provided copious amounts of invaluable skills and experience. His leadership over the Blast and Impact Dynamics Laboratory is an incredible example of his commitment to leading students to success beyond the classroom. Mr. Matt Lowe and Mr. Brad Ferguson deserve great thanks for their graciousness with their time and space in the Mechanical Engineering Machine Shop. Mr. Brad Ferguson used his expert machining skills to cut incredibly precise samples from rods used in this experiment to aid in the quality of test results. Several undergraduate students involved in the Blast and Impact Dynamics Undergraduate Research group provided invaluable help during the setup, testing, and analysis of the sample. Most notably, Courtney Cruse, Katherine Terry, and Isabella Scalia. Their skill and time under the supervision of Dr. Damian Stoddard does not go unnoticed. Stanford White IV should also be thanked for his incredible work in creating a software to be used in the experimental analysis. Finally, the author would like to thank all her family and friends for their unwavering encouragement.

ABSTRACT

The Effects of UV Degradation on Polycarbonate Plastics Under Dynamic Compressive Loading

The objective of this experiment was to analyze the dynamic properties of polycarbonate plastics subjected to accelerated ultraviolet (UV) exposure. This was done by subjecting rods of polycarbonate plastic to UV degradation in a QUV accelerated weathering machine for 375, 750, and 1500-hours. These rods were then tested under dynamic compression using a Split-Hopkinson Pressure Bar at an average strain rate of 1600/s. The Split-Hopkinson pressure bar works by rapidly compressing a sample between 3 axial rods sending an elastic wave through the sample. The strain gauges on the incident rod and the transmission rod transformed the elastic wave deformation into a voltage change that was then converted to stress and strain values. This allowed for an analysis of the dynamic response of the samples under compressive conditions. The samples were compared with a control group of polycarbonates to better understand the effects of UV degradation.

The results of this experiment showed little change in the material response for the control, 375, and 750-hour UV exposure sample groups. This indicates that 750 hours of accelerated UV exposure was not significant enough to cause changes in the Polycarbonate sample properties. 1500-hour sample groups showed an increase in plateau strength as compared to the other sample groups with a value of 169.03 MPa which was 35.5% more

than the control group plateau stress. The energy density of the samples described the amount of energy absorption per unit volume of the sample and the trend was the same as for the plateau strength. The changes in properties were indicated by the 32.6% increase in energy density for the 1500-hour samples with a value of 37.54 kJ/m^3.

TABLE OF CONTENTS

LIST OF TABLES/FIGURES

List of Tables

List of Figures

INTRODUCTION

Poly Carbonate:

In order to understand this experiment it is important to first understand polycarbonate, the material being studied. Polycarbonate is a thermoplastic considered to be one of the fastest growing engineering plastics (British Plastics Federation). Polycarbonate (PC) was discovered in 1898 when a German Chemist, Einhorn, was working to prepare cyclic carbonates by reacting hydroquinone with phosgene and observed the formation of an infusible, insoluble solid. Bischoff and Hedenström found a similar cross-linked, high-molecular-weight PC in 1902. In 1953, Bayer laboratories began producing linear thermoplastic high-molecular weight Polycarbonate. Finally, in 1960 both Bayer and General Electric began commercial production of the material (British Plastics Federation).

Polycarbonate is used in a large variety of markets including the automotive, electronic, glazing, optical media, business machine, medical, lighting, and appliance markets (British Plastics Federation). Polycarbonate is even becoming increasingly popular in the building industries. PC has low cost and is easy to use compared to materials like glass, metal, wood, and mortar of which the polycarbonate can replace in many applications (Yousif & Haddad, 2013). Some other applications for polycarbonate include protective coatings, aeronautics, agricultural greenhouses, and marine vessel hulls. Each of the applications mentioned indicates how large scale of an impact Polycarbonate has on

the modern world, and this is only predicted to increase. The market is expected to expand at a compound annual growth rate of 3.5% from 2023 to 2030 (Grand View Research, 2021).

UV Weathering:

Understanding the mechanical properties of Polycarbonate is crucial given its wide-ranging applications and the projected market growth. Plastics exhibit a wide spectrum of mechanical behaviors, ranging from brittle to ductile materials, depending on their composition. Thus, studying the specific responses of different plastics under varied environmental conditions is imperative for comprehending their characteristics and utility. One significant concern is the rapid photodegradation of polymeric materials when exposed to natural weathering.

Objects and materials in the physical environment are inevitably subjected to external atmospheres and weather conditions, leading to various forms of weathering. The severity of these effects depends on both the harshness of the surroundings and the intrinsic properties of the materials. Factors such as heat, moisture, and wind play pivotal roles in determining the extent of weathering (McKeen, 2013). Numerous studies have investigated the degradation of materials due to these components, recognizing its profound implications on both the aesthetic appeal and structural integrity of materials, thereby influencing economic and environmental factors. Considering these weathering components and their impacts is crucial during design and analysis phases. Yousif and Hadad (2013) defined degradation of macromolecules to describe any process leading to the decline of polymer properties. This decline could affect the material physically through

polymer recrystallization or chemically by reducing or increasing the average molar mass through macromolecular chain bond scission or crosslinking. Varying temperatures and humidities, rain, wind, pollutants, atmospheric gases, and light are different weather components that can affect a material. The study conducted in this report focuses on the effects of ultraviolet (UV) rays that are present in sunlight.

Sunlight is one of the most important components of degradation. Light emitted from the sun's rays comes in different wavelengths which describes the distance from peak to peak of their sinusoidal wave shape. Visible light describes the light emitted in rays of wavelengths between 400 and 780nm. This is the light that can be seen. The electromagnetic spectrum (Figure 1) provides a clear visual of the transition of wavelengths sizes into the different forms of lights.

Wavelengths shorter than those in the visible light spectrum are not seen by the human eye but still have important impacts. In fact, a large percentage of damage to durable materials exposed outdoors is caused by short wavelength ultraviolet light even though UV light only makes up around 5% of sunlight (McKeen, 2013). This is because UV light emits enough energy to cause chemical changes in polymeric chains (McKeen, 2013).

UV light ranges from 100nm to 400nm wavelengths split up into three different categories: UV-A, UV-B, and UV-C. UV-C describes the ultraviolet light with the smallest wavelengths and UV-A is the ultraviolet light with larger wavelengths. UV light was discovered in 1801 by Johann Ritter while he was investigating colors beyond violet in the light spectrum. He exposed photographic paper impregnated with silver chloride to light beyond violet and it caused the paper to turn black (Science Mission Directorate, 2010).

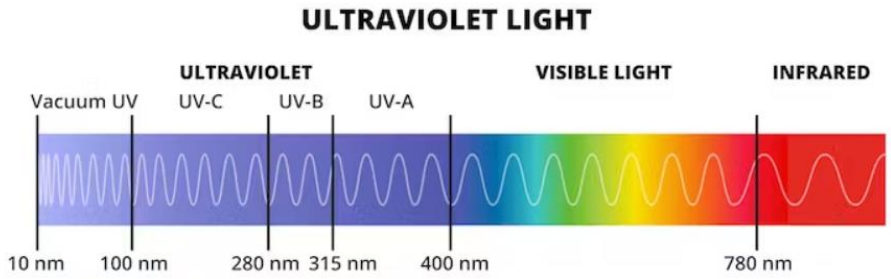

Figure 1. Light Spectrum (Lotti Tajouri Associate Professor et al., 2023)

Bonds are not broken when light of longer wavelengths at any brightness or intensity contact a material, but shorter wavelengths at any intensity can break the bond. This macromolecular chain bond scission merits concern in design and other considerations. UV C defines wavelengths between 100 and 280nm. The short wavelengths making up UV C mean that it is the most damaging type of UV light. According to Mckeen, shorter wavelengths indicate more energetic light (McKeen, 2013) (sunlight, uv, and accelerated weathering). However, UV C is completely absorbed by the Ozone layer blocking the negative impact that this UV light could have on people and objects in earth's atmosphere. UV B defines ultraviolet wavelengths between 280 and 315nm. UV B is mostly absorbed by the ozone layer and can also cause significant damage. UV B that is not absorbed by the ozone layer can cause severe polymer damage. UV A (315-400nm) is the ultraviolet light that passes through the ozone layer the most, so it can affect materials in earth's atmosphere to the greatest extent. This causes it to be of primary concern in natural weathering (McKeen, 2013).

Additives:

As previously mentioned, changes in chemical bonds in the plastics due to this UV light could result in very serious economic and environmental implications. The economic

implications are in part due to loss of aesthetic appearance caused by yellowing. This could change the marketable value of an object. The effects of light to the structural integrity of a material also causes economic damage as measures should be made to ensure the quality of a material being used in production is to standard. The aesthetic and structural risks are worth understanding and preventing because of the magnitude of their repercussions.

Many tests have been made on the impacts of UV light on various materials and chemical studies have been performed to produce additives that can reduce the UV chemical, physical, and aesthetic damage. The additives can be added to a material in different ways such as a co-extrusion process. This process works to create an optimally balanced set of properties through extruding two or more materials through a single die (British Plastics Federation). In this experiment, the polycarbonate rods used had an ultraviolet resistant additive on them. The nature of the additive is unknown.

Split Hopkinson Pressure Bar:

There are many different material and engineering testing techniques that could be implemented in order to understand the effects that the accelerated UV degradation had on the polycarbonate samples. For this experiment, dynamic compressive testing was of primary interest. Dynamic testing of a material is a test that helps give information on the dynamic response of a material. Blast and impact testing encapsulates this dynamic testing, and it ranges from tests performed at a strain-rate of between 10 and 10^6 per second. Different test methods have been developed to test materials at varying strain-rates. Figure 2 presents a visual of the different types of strain-rates experienced by materials during different loading events. Materials behave differently when loads are applied at different

rates. A material may act one way under a static load and have a dramatically different reaction when the load is applied at a high strain-rate. It is important to study dynamic compressive testing to better understand materials used in applications such as armors, protective systems, and other dynamically loaded materials.

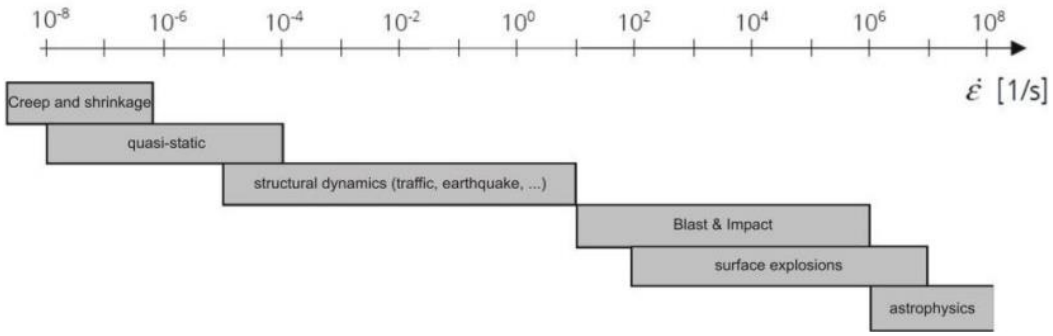

Figure 2. Strain-rates for different loading events (Federoff et al., 2017)

In this experiment, dynamic compression testing was performed using the Split-Hopkinson Pressure Bar (SHPB) or Kolsky bar which was invented in 1962 by Bertram Hopkinson and Herbert Kolsky (*ASME* 2006). The SHPB is a piece of material testing laboratory equipment used to understand a material's response to dynamic loading in the form of either compression or tension by performing high strain-rate material characterization to obtain the properties of a material. The equipment is equipped with a series of three axial rods (figure 3). A barrel on one end of the rods is pressurized to a desired psi. The pressure is released using a pneumatic launcher causing a striker rod inside the barrel to encounter the incident rod sending an elastic wave propagating through the rod. The sample is sandwiched between the incident rod and the transmission rod. The elastic wave propagates through the material sending some of the wave through the transmission rod and reflecting a portion of the wave back across the incident rod. A SHPB setup can utilize many different materials for the bars, provided that the material is

consistent across the three rods, and they are the same diameter. There must be some impedance difference between the SHPB bars and the samples being tested in order to produce the reflected wave back through the incident bar. This can be accomplished by using a smaller sample diameter than the diameter of the rod and/or using a different bar material than the sample being tested. It is also important to ensure that the bar material has an equal or lower strength value than the sample so as to not damage the equipment during dynamic compression. The strain gauges attached to the incident and transmitted rods convert the elastic deformation in the rods into voltage readings that can provide stress and strain data for the sample.

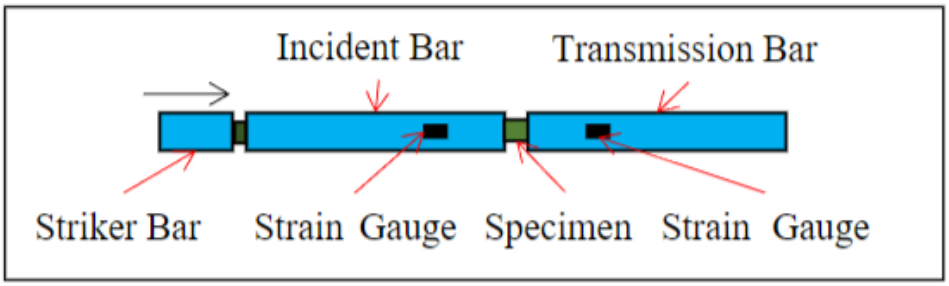

Figure 3. Basic schematic of a SHPB experimental setup (Stoddard et al., 2020)

Strain Gauging:

Strain gauging is a technique used to accurately measure strain through electrical resistance. Strain gauges were invented in 1938 by Edward E. Simmons and Arthur C. Rose. They are a measuring tool composed of wires, insulating backing, connecting terminals, and a thin metallic foil as shown in figure 4. The thin metallic foil on the gauge causes a change in resistivity through the wire during deformation as the gauge deforms with the object during applied force. Ohm's law (equation 1) relates the change in resistance experienced by the strain gauges from the deformation to a voltage output from

the loading. Figure 5 shows the process of strain gauging deformation and the effects it has on resistance.

$$V=IR \qquad (1)$$

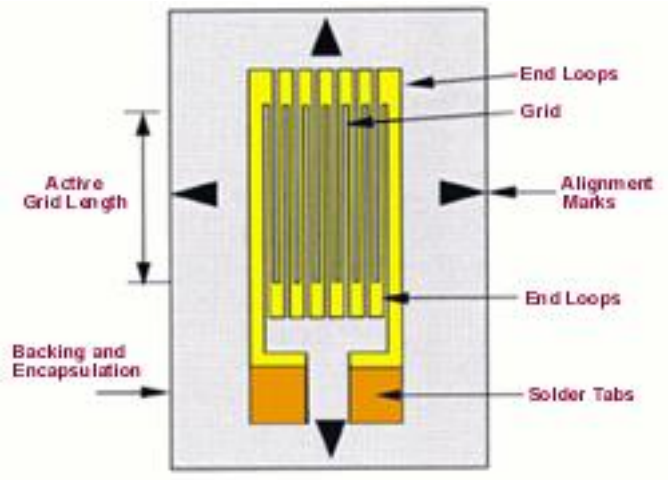

Figure 4. Metallic Foil Stain Gauge Components (P. Raju Mantena, 2012)

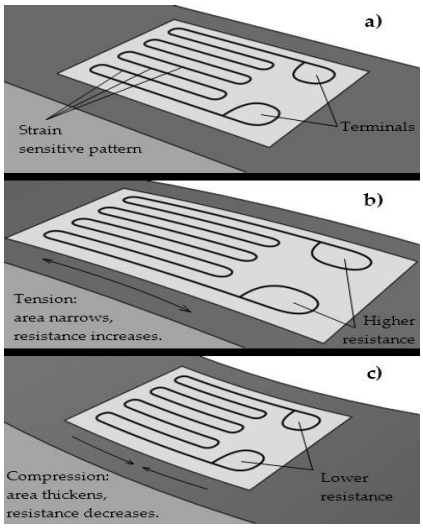

Figure 5. Metallic Foil Electrical-Resistance Strain Gauge (P. Raju Mantena, 2012)

Stress analysis through strain gauging is a very important process and concept in engineering and in understanding the effects of loading, tension, and compression in general. Stress and strain values are very important for engineering design. These values provide insight into many other characteristics of a material such as yield strength, ultimate tensile strength, plastic deformation range, cross-sectional area, and the young's modulus of a material. This can be seen in that engineering strain (ε) is a reaction of a material to an applied stress and is defined as the change in length in the direction of the applied force divided by the original length (equation 2). This value is related to stress σ and the young's modulus E of a material through Hooke's law where $\sigma = E\varepsilon$. Similarly, stress is related to load (P) and the original cross-sectional area (A_0) of the material through equation 3 . The combination and calculation of each of these values allows engineers to design structures according to the expected loads and desired reactions of the materials whether that be resist fracture or resist plastic deformation.

$$\varepsilon = \frac{l - l_0}{l_0} \qquad 2$$

$$\sigma = \frac{P}{A_0} \qquad 3$$

One important concept to understand when dealing with the strain gauging technique is the Wheatstone Bridge configuration of a circuit as seen in figure 6. This configuration is used to measure the change in resistance due to strain. As the strain gauge deforms and causes changes in the electrical resistance, the Wheatstone bridge circuit creates a differential voltage variation. This change in voltage can then be calibrated to

correspond to the physical force applied to the gauge and calculated through the load cell circuit voltage output.

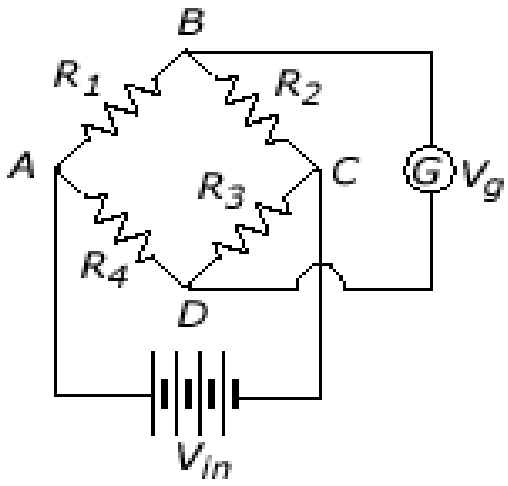

Figure 6. Wheatstone Bridge Configuration (P. Raju Mantena, 2012)

As seen in figure 6, a Wheatstone bridge contains four resistances, a voltage input (Vin), and an output voltage gauge (Vg). These components are related to each other by equation 4.

$$V_g = \frac{R_1R_3 - R_2R_4}{(R_1 + R_2)(R_3 + R_4)} V_{in} \quad (4)$$

If R1R3=R2R4 or R1/R2=R4/R3=1/r then the output voltage will become zero and the bridge is balanced. Any change in strain due to loading will affect the resistance balances and the voltage change can be calculated from equation 5.

$$\Delta V_g = V_{in} \frac{r}{(1+r)^2} \left(\frac{\Delta R_1}{R_1} - \frac{\Delta R_2}{R_2} + \frac{\Delta R_3}{R_3} - \frac{\Delta R_4}{R_4}\right) \quad (5)$$

There are three configurations that fall under the Wheatstone bridge category, the quarter bridge, half bridge, and full bridge configurations. The quarter bridge configuration was used for the SHPB setup to cancel out bending. Strain gauging is a highly accurate method for calculating resistance changes and thus strain so its application for Split-Hopkinson Pressure Bars is very effective. It is highly accurate, cost effective, and reliable long-term.

MATERIALS AND METHODS

The Polycarbonate used for this experiment was ordered from McMaster Carr and was produced with a UV resistant additive of an undisclosed makeup. The PC was shaped in rods 18” long with ¼” diameter and then machined into ¼” by ¼” samples to be compressed in the SHPB. This was done in the University of Mississippi Mechanical Engineering machine shop using a lathe. Figure 7 shows an image of two polycarbonate treated and controlled samples before testing.

Figure 7. Polycarbonate treated and control samples before testing

A QUV accelerated weathering machine (figure 8) was used to subject the plastics to Ultraviolet Light exposure for three different durations of time. The QUV machine is a widely used accelerated weathering test machine and it was designed to replicate various weathering conditions by reproducing the damage caused by the sunlight, rain, and dew. This experiment was interested in the effects of UV so the system was only setup with fluorescent UV lamps. The lamp used was a 340nm UV A bulb that emits UV light at

wavelengths between 295nm-365nm. Figure 9 shows the polycarbonate samples placed in the QUV machine near the fluorescent lamp.

Figure 8. QUV Accelerated Weathering Tester

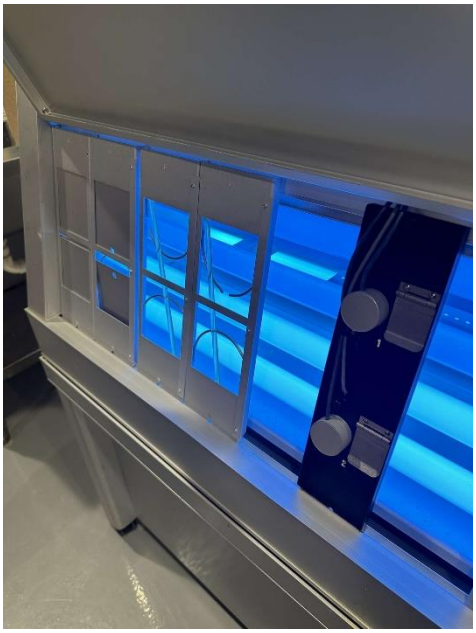

Figure 9. Polycarbonate Rods in QUV Accelerated Weathering Tester

The rods in this experiment were placed in the QUV machine at 0.68 $\frac{W/m^2}{nm}$ for a determined number of hours. The control group rod did not experience any UV exposure from the QUV machine and was securely stored in a box to reduce possible weathering exposure. The other 3 rods were placed in the machine for 375, 750, and 1500 hours. These hours correspond to 15.62, 31.25, and 62.5 days respectively.

An article by Shokrieh and Bayat helps explain how the accelerated weathering machine UV degradation hours correspond to natural sunlight. This article uses the UV outdoor dosage in the state of Florida for comparison and it states that the UV outdoor dose for a year in Florida is 280 x $10^6 \frac{J}{m^2}$. Equations 6 and 7 present the equations used to convert the accelerated degradation hours to estimated natural sunlight exposure. Equation 6 calculates the UV dosage in $\frac{J}{m^2}$ that the accelerated weathering machine emitted given a UV intensity of 230 $\frac{w}{m^2}$ from the fluorescent bulb used in this experiment. This number was compared to the yearly UV dosage in Florida recorded in the article by Shokrieh and Bayat. The sample calculations provided indicate that that an exposure time of 750 hours in the accelerated weathering machine using a fluorescent bulb corresponded to approximately 2.2 years of UV dosage in Florida. Table 1 presents a rough value for the comparison between the accelerated weathering machine and UV exposure in Florida (Shokrieh & Bayat, 2007). The table lists the QUV accelerated weathering machine fluorescent bulb time in hours, the approximate real time based on values in Florida in hours, and then the value converted into units of years. When comparing the hours, a roughly 25% increase was calculated between the accelerated time and its equivalent real time.

Table 1. Comparison between accelerated UV weathering machine exposure hours to hours in Florida

QUV accelerated weathering machine (hours)	Estimated time (hours)	Estimated time (years)
375	9714	1.1
750	19428	2.2
1500	38857	4.4

$$Exposure\ Time = \frac{UV\ dosage}{UV\ intensity} \quad (6)$$

$$375hrs * 60\frac{min}{hour} * 60\frac{s}{min} = \frac{UV\ dosage}{230\ \frac{W}{m^2}}$$

$$\text{UV dosage} = 621x10^6\ \frac{J}{m^2}$$

$$years\ in\ Florida = \frac{UV\ dosage}{Yearly\ UV\ dosage\ in\ Florida} \quad (7)$$

$$years\ in\ Florida = \frac{621x10^6\ \frac{J}{m^2}}{280x10^6\ \frac{\frac{J}{m^2}}{yr}}$$

$$years\ in\ Florida = 2.2\ \text{years}$$

It is important to note that there are many factors involved in weathering and these numbers are only rough estimates. The amount and spectrum of natural UV exposure is extremely variable because it is easily altered by cloud cover, pollution, air mass, and location on earth's surface. The QUV machine can only address a specific set of conditions because of the many factors involved in climate conditions. Accelerated weathering

machines aim to reproduce the damaging effects of sunlight, not sunlight itself (Sunlight, UV, and Accelerated Weathering).

THEORY/ANALYSIS

A Split-Hopkinson Pressure Bar compression technique uses a series of three axial rods, a striker rod, incident, rod, and transmitted rod. The striker rod generates an elastic stress wave through the incident rod when the desired pressure built up in the pneumatic launcher is released. This sends the striker rod to make direct contact with the incident rod. The elastic wave propagates through the sample that is sandwiched between the incident and transmitted rods sending some of the wave through the transmitted rod and reflecting a portion of the wave back through the incident rods. This is shown visually in figure 10 with a schematic of the experimental setup along with a visual of the wave propagation through the rods. It was important that the sample and the rods were made from different materials so that they experience different stress values, and the sample maximum stress did not surpass the yield strength of the bar. Strain gauges mounted on the incident and transmitted rods record the bar response to the elastic wave motion through the gauges to provide important information regarding the dynamic response of the sample (Stoddard et al., 2020).

The direct data recorded from the sample experiment provided a voltage reading sent out from the strain gauges. The measured voltage change was able to be directly translated to the strain response in the rods at either end. Data processing was done using an in-house analysis software. This software performs the stress-strain analysis from the voltage readings in a python script

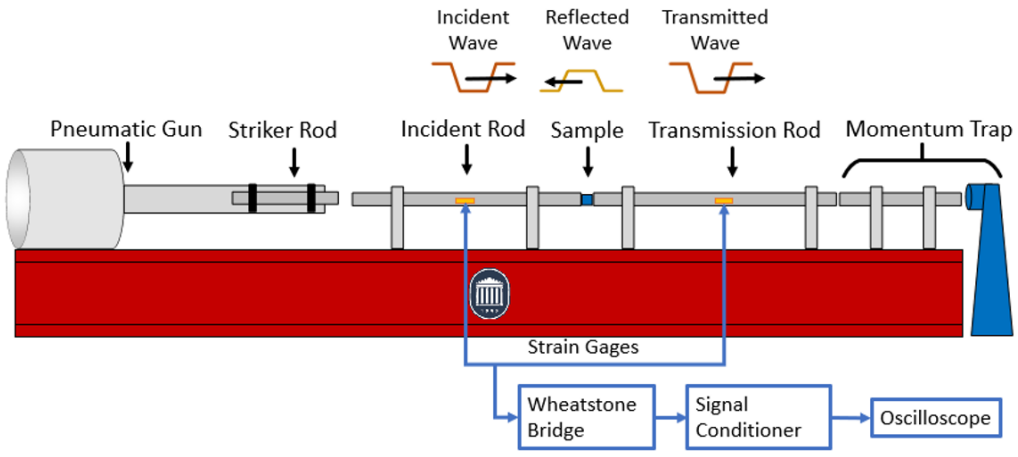

Figure 10. Split-Hopkinson Pressure Bar experimental setup (Turner, 2019)

To ensure validity of the test results, the force at the end of the incident rod must be equal to the force at the end of the transmission rod. After equation simplifications, the stress equilibrium condition could be simplified to equation 8 where ε_i , ε_r , and ε_t indicate the instantaneous strain response in the incident rod, reflected wave, and transmitted end respectively.

$$\varepsilon_i + \varepsilon_r = \varepsilon_t \qquad 8$$

After ensuring test validity, the sample strain could be found in terms of the reflected strain using information on the displacement at the ends of the bar and the relationship between the incident, reflected, and transmission strains (equation 9). C_o referred to the elastic wave speed and L_s referred to the length of the sample. This also allowed for the calculation of the strain-rate at any point during the experiment (equation 10).

$$\varepsilon_s = \frac{-2C_o}{L_s}\int_0^t \varepsilon_r \, dt \quad (9)$$

$$\dot{\varepsilon}_s = \frac{-2C_o}{L_s}\varepsilon_r(t) \quad (10)$$

Correspondingly, the stress in the sample could be obtained using equation 11. E_b is the elastic modulus of the bar and A_b and A_s are the cross-sectional area of the bar and the sample respectively.

$$\sigma_s = E_b \frac{A_b}{A_s}\varepsilon_t(t) \quad (11)$$

A more in-depth explanation of the SHPB analysis theory can be found in an article by Stoddard et al. titled "High Strain-rate Dynamic Compressive Behavior and Energy Absorption of Distiller's Dried Grains and Soluble Composites with Paulownia and Pine Wood Using a Split Hopkinson Pressure Bar Technique".

EXPERIMENTAL SETUP

The dynamic response test that was performed for this experiment utilized an REL Split Hopkinson Pressure Bar in the Blast and Impact Dynamics Laboratory at the University of Mississippi (Oxford, MS, USA) to rapidly compress the polycarbonate samples (Stoddard et al., 2020). The SHPB was equipped with three aluminum axial rods with material properties as listed in table 2. The Polycarbonate samples were placed securely between the incident and transmitted rods as seen in figure 11. Each of the samples were impacted with a pressure of 20 psi from the barrel incorporating a fixed strain-rate into the experiment.

Table 2. Properties of the Aluminum bars used in the experimental setup

Young's Modulus (GPa)	68.9
Density (kg/m^3)	2700
Diameter (m)	0.019

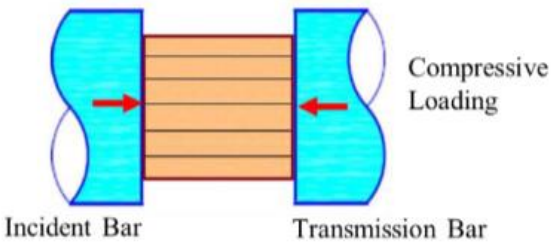

Figure 11. Dynamic Compressive Loading of the Polycarbonate (Stoddard et al., 2020)

A Shimadzu HPV-2 (Shimadzu Corporation, Kyoto, Japan) high-speed video camera was used to capture the full deformation/failure process. The camera was set to a fixed resolution of 312 pixels × 260 pixels and a recording speed of 250,000 frames per second (fps). This component of the experimental setup provided clear visual images of the sample deformation across time to further understand the dynamic response of the polycarbonate.

RESULTS AND DISCUSSION

The direct results from this experiment came from information on the force experienced by the strain gauges fixed to the incident rod and to the transmission rod through the duration of the experiment. For this experiment to be valid, it was important for each test to have reached stress equilibrium. To check the validity of SHPB results, the stress uniformity conditions were determined for each experimental configuration. Stress equilibrium ensured uniform material characteristics from the test by ensuring similar bar end forces on either end of the specimen (Wu & Gorham, 1997). To check stress equilibrium, a plot of force vs time for each sample in each UV exposure time span was plotted. Figure 12 depicts the plot of Force vs time for sample 1 of the polycarbonate samples subjected to 1500 hours of UV exposure in the QUV accelerated weathering machine. This figure shows three different curves describing the force on the incident end, the transmitted end, and the averaged values. The figure shows that the overlayed force vs time curves on either end line up very closely to the average value and to each other. This demonstrates stress equilibrium for the data recorded for this sample. Stress equilibrium was plotted for each sample tested in this experiment and the figures indicated excellent results across the board. This validated the data from this experiment and added confidence to the subsequent calculations performed and figures plotted.

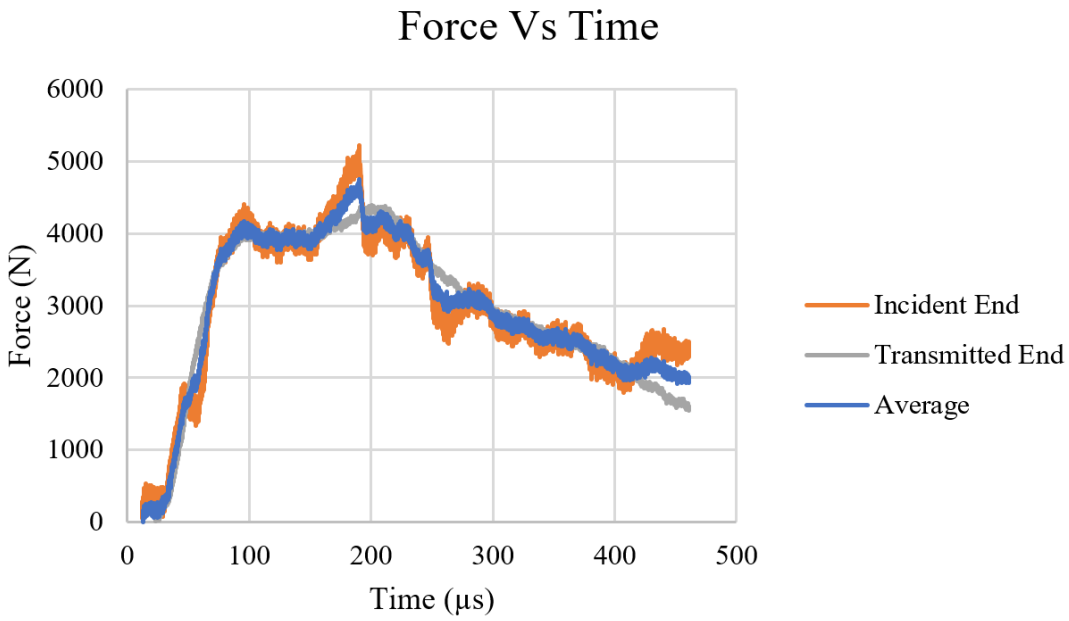

Figure 12. Force vs Time for sample 1 of the 1500 hour UV degradation exposure group

Figures 13-16 present the stress vs strain plots for each group of UV degradation exposure times. Each plot contains data curves corresponding to the different samples tested from that group. Figure 13 presents the stress and strain for the control group of polycarbonate plastics. The control group was not subjected to the accelerated weathering from the QUV accelerated weathering tester. This figure shows that the test resulted in similar results across samples. This indicates that each sample of the polycarbonate plastics in the control group behaved similarly under dynamic compression, further adding confidence to the result validity and in the material properties determined using this information.

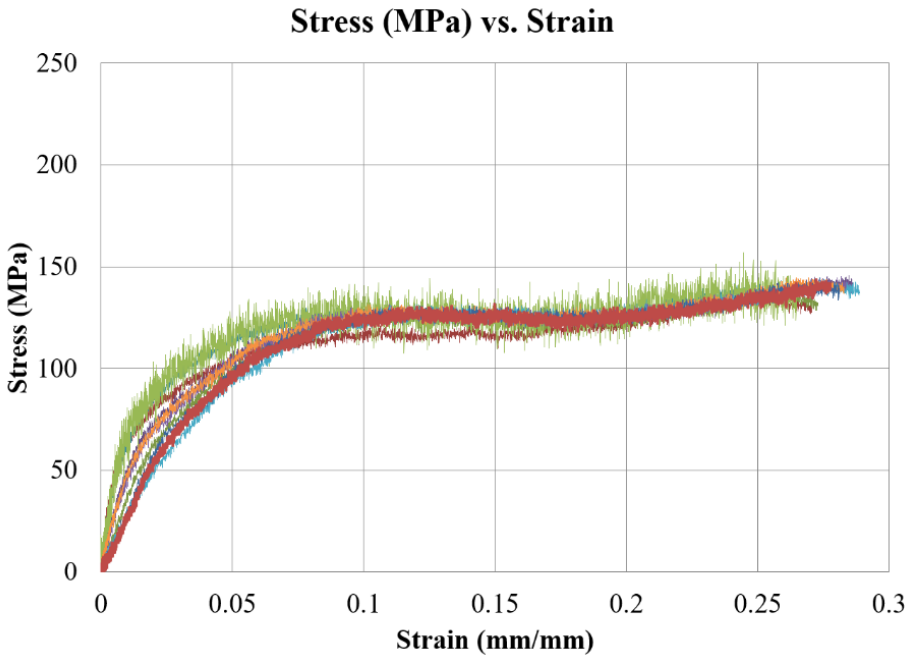

Figure 13. Stress vs strain curve for the control group

Figure 14. presents the stress vs strain curve for the polycarbonate samples subjected to UV degradation under the fluorescent bulb for 375 hours. This curve shows a similar trend to the control group. The different samples all resulted in consistent trends helping prove accurate testing data and procedure. The trend of the figure shows a rapid increase in stress until approximately 5% strain where the stress values began to level out with little additional stress experienced by the sample even as strain increased. This is called plastic flow .

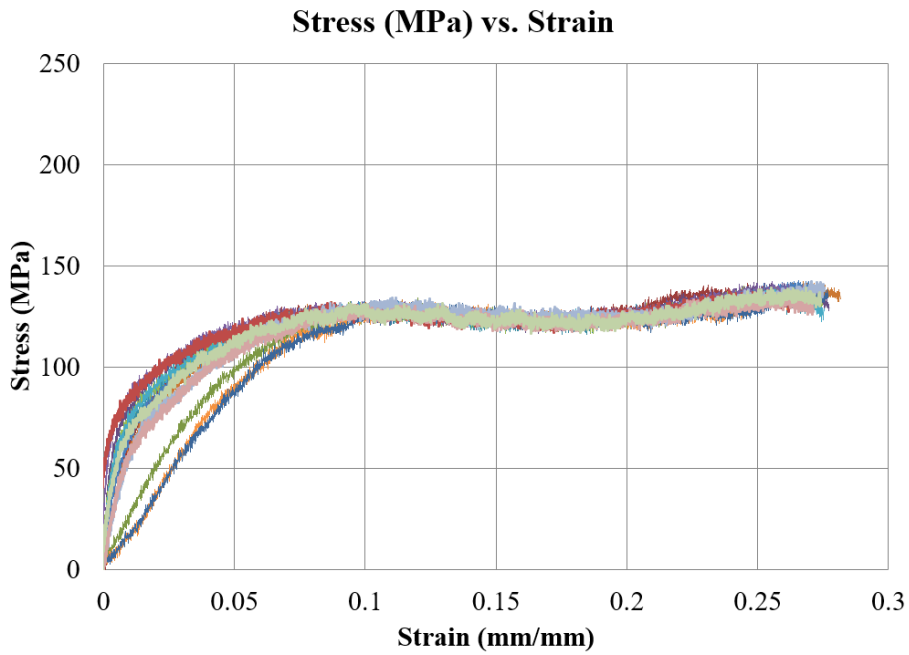

Figure 14. Stress vs strain curve for the 375 hr UV exposure group

Figure 15. presents the stress vs strain curve for the samples subjected to 750 hours of UV degradation. This figure appears to be very similar to the stress vs strain curves plotted for the previous UV exposure groups. This indicates that the 375 hour increase in UV exposure from the QUV accelerated weathering machine equipped with UV A fluorescent bulbs as compared to the previous sample group did not have a significant impact on the dynamic stress-strain relationship. These results suggest that if the UV exposure is to cause any significant changes to the properties of the sample, a longer accelerated UV exposure time is necessary.

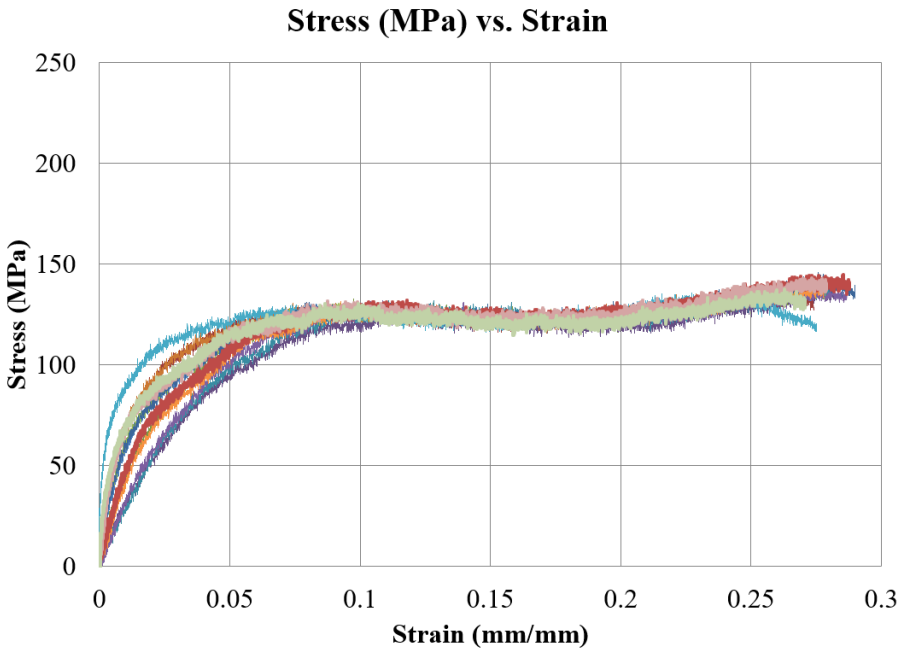

Figure 15. Stress vs strain curve for the 750 hr UV exposure group

Finally, figure 16. presents the stress vs strain curves for the longest period of accelerated UV exposure experienced by the polycarbonate samples. These plastics were exposed to UV light from the fluorescent bulbs for 1500 hours which approximately corresponds to a true UV exposure of 4.4 years in Florida. The plot shows consistent data across the 15 samples and very little noise within each curve. Interestingly, this curve shows higher plateau stress values than was displayed for the samples exposed to shorter durations of UV light. This indicates an increase in strength as the UV exposure time increased. This appears to go against ideas regarding UV degradation and the experimental hypothesis that UV light would degrade the plastics over time, however, this trend could point to the gradual embrittlement that is often experienced by plastics placed in the sun. Brittle materials are characterized as having a high compressive strength and a low tensile strength (Zhang, 2011). Plastics becoming more and more

brittle would have an initial increase in strength. An explanation for this phenomenon would be that it would be compromising its structure by losing its toughness.

The limitations of this experiment did not allow the PC samples to be tested to failure to explore the dynamic compressive response failure conditions. The samples did not reach compressive failure in part due to the length of the striker rod. The duration of the experiment directly correlates to the length of the incident rod so the size of the rod used in this experiment was not sufficient to induce compressive failure. Instead, figures 13-16 show the stress-strain data until a plateau strength was reached. Each of the UV exposure times plotted in figures 13-16 display a similar trend of rapid increase in stress until past 5% strain where the curve then depicts a plateau of stress value. Were this to be a representation of the gradual embrittlement of the PC exposed to UV light, this plateau strength would be indicative of the high compressive strength of brittle samples. Further studies should be done to explore this hypothesis for these experiment parameters.

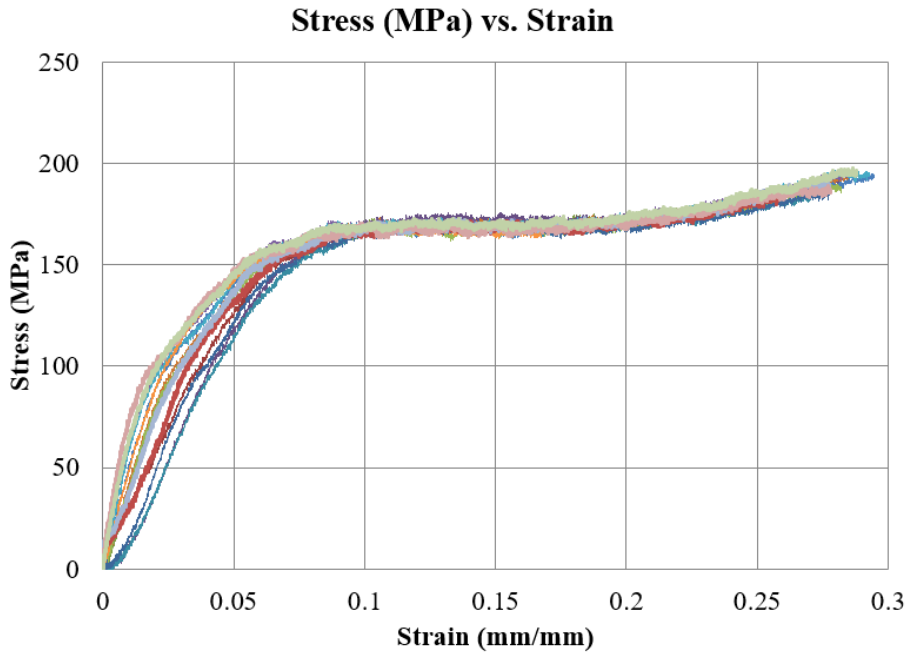

Figure 16. Stress vs strain curve for the 1500 hr UV exposure group

The plateau strengths graphically displayed in figures 13-16 are numerically tabulated in Table 3. The table clearly shows that the plateau strengths for the control group, 375-hour UV exposure group, and the 750-hour UV exposure group saw very little change in the plateau strength of the samples. The control group had a plateau strength of 124.73 MPa and the 750-hour UV exposure group had an average plateau strength of 123.40 MPa which was a 1.07% difference in comparison to the control group. Table 3 does show a noticeable difference in the plateau strengths of the 1500-hour samples. The average stress was 169.03 MPa which was a 35.51% increase from the control group.

As was discussed previously, this correlation between the increase in strength values to the increase in UV exposure time could be accounted for by a gradual embrittlement in the plastics. This could be explored further by exposing the plastics to longer periods of UV exposure and incorporating a testing method that tests the samples to failure.

Table 3. Plateau Strength Comparisons for each UV exposure time

Hours	Plateau Strength (Mpa)	Control Comparison (%)
Control	124.73	---
375	124.49	0.19
750	123.40	1.07
1500	169.03	35.51

Figure 17 presents an Energy Density vs Strain plot. The plot has 4 curves belonging to the different UV exposure time span groups overlayed for comparison purposes. Energy density is a value that describes the energy absorbed per unit volume and is found by calculating the area under the stress-strain curve using equation 12. The figure

shows that the curves corresponding to the control, 375, and 750 hour samples were similar. Their overlayed curves followed a very similar trend. The outlier was the blue curve that corresponded to the samples exposed to 1500 hours of fluorescent bulb UV A exposure. This curve indicated an overall higher energy density value at the different strains as compared to the other samples. The 1500-hour samples absorbed more energy per strain. It is interesting to note, however, that there was a crossover from the blue curve across the other curves at the lower strain values. This suggests that until around 7.3% strain, the plastics experienced the same amount of energy absorption capabilities at which point the 1500-hour samples superseded the energy density of the other plastics. This was perhaps suggestive of the compressive strength brittle properties caused by the UV. Similarly, 7.3% strain on the stress strain curve corresponded to a point on the curve where the samples experienced a significant change in stiffness from a stiffer response to a softer response indicated by the softening region

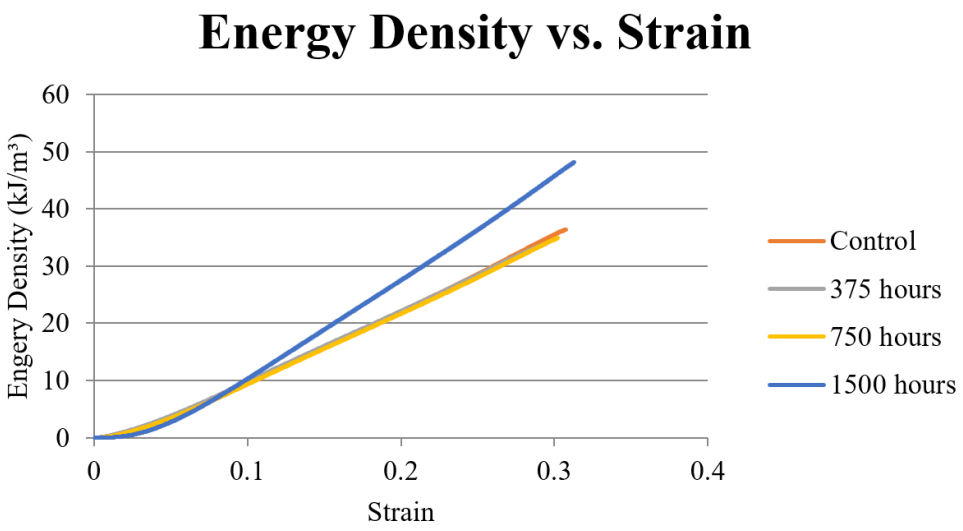

Figure 17. Energy Density vs Strain for control group, 375, 750, and 1500 hr samples

$$U^* = \int_0^{\varepsilon} \sigma d\varepsilon \qquad 12$$

Table 4 displays a comparison of the energy density values for 0.25 strain for each UV exposure time span. The table numerically quantifies the trend displayed in figure 17. Similar to the data for the plateau strength, the values for the control samples, 375 hour samples, and 750 hour samples were very similar. The energy density for the control samples at 25% strain was 28.30 kJ/m³ and the energy density for the 750 hour samples was 28.46 kJ/m³ which was a 0.58% difference from the control group. The similarities between those three sample groups further indicates that 750 hours of accelerated exposure was not significant enough to report a change in the properties of the material as indicated by the energy absorption per unit volume recorded in table 4. The energy absorption of the PC exposed to 1500 hours did indicate a change in the properties of the samples. The value was 37.54 kJ/m³ which was a 32.64% increase from the control group.

Table 4. Energy Density values at 0.25 strain for each UV exposure time

Hours	Energy Density (kJ/m³)	Control Comparison (%)
Control	28.30	---
375	28.94	2.27
750	28.46	0.58
1500	37.54	32.64

A before and after picture of the polycarbonate samples in the experimental setup is presented in Figure 18. These photos were captured using the Shimadzu High-Speed

camera at a frame rate of 250,000 fps. Prior to compression, the samples were ¼” by ¼” in size. After compression, the sample experienced shape deformation producing a barrel shape.

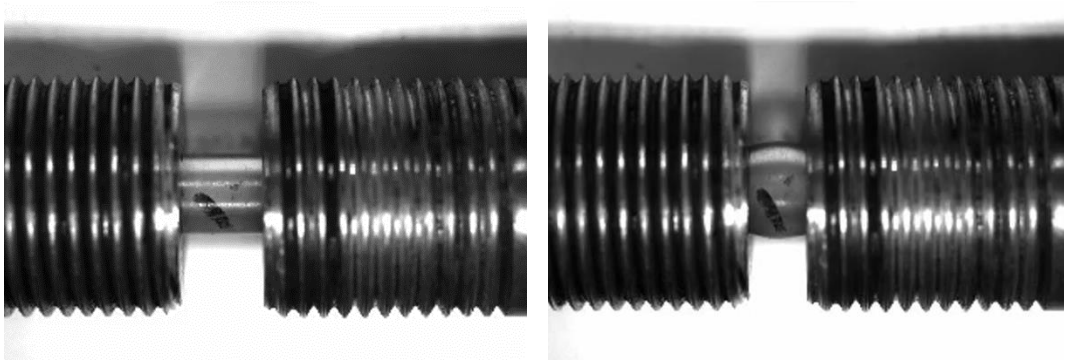

Figure 18. 1500 hr sample 8 before and after compression

To further understand the relationship between the UV exposure time and both the plateau strength and energy density figures 19 and 20 were plotted. Figure 19 presents the average plateau strength for a specified strain range vs the UV exposure time in hours. Figure 20 presents the energy density at 25% strain plotted vs the UV exposure time. Visually, both figures appear to be very similar. They follow the same trend of little variation in plateau strength until 750 hours where the properties increased. This trend indicates that longer exposure time could provide more information on the effects of UV accelerated weathering on the Polycarbonate.

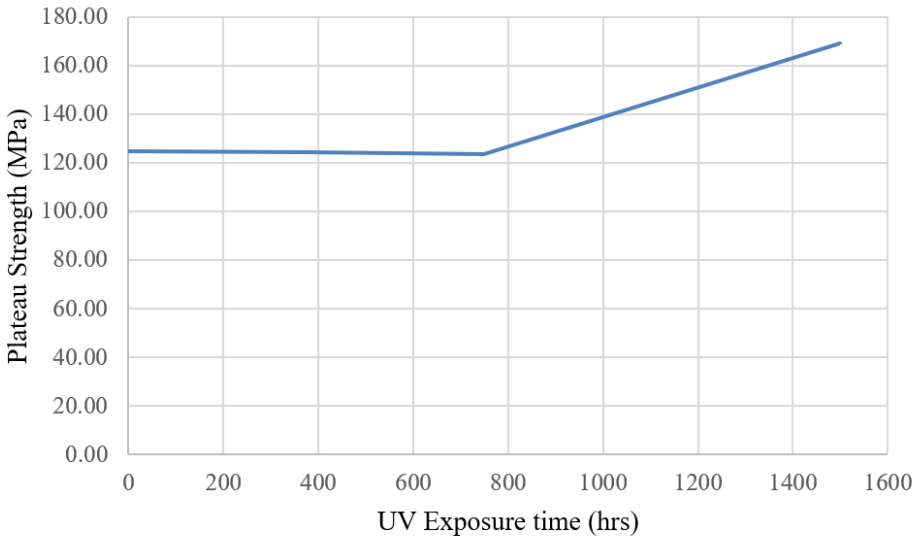

Figure 19. Plateau Strength-UV exposure time comparison

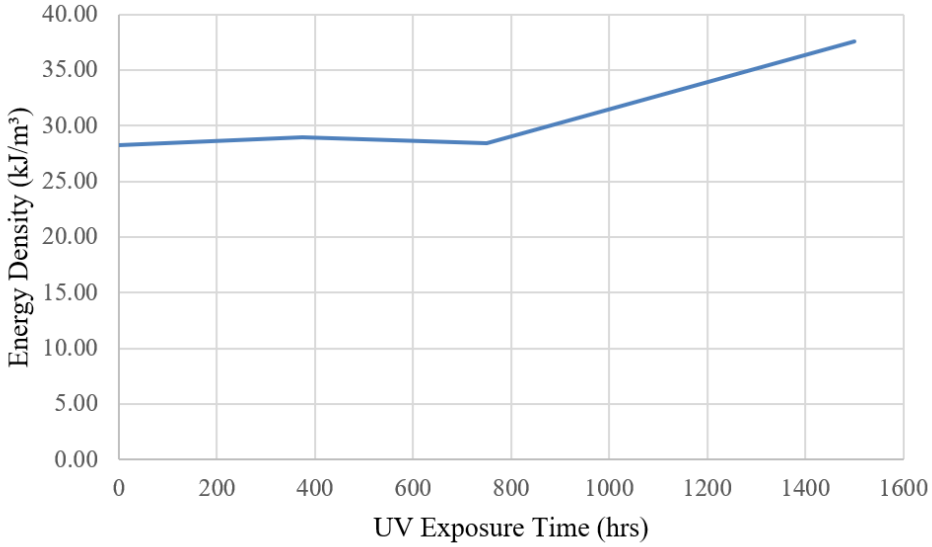

Figure 20. Energy Density at 25% strain-UV exposure time comparison

An article by Brown was useful in understanding the brittle nature of plastics and in further understanding the discovered results from this experiment. In this article, Brown supported the idea that brittle polymers have lower flexibility and higher strength due to their stronger intermolecular bonding (Brown et al., 2009). In the case of this

experiment, the UV degradation applied to the plastics worked to begin breaking down the chain bonds and could have begun making the polycarbonate rods more and more brittle. This would have shown up in the stress-strain graphs by indicating higher strength in the compressive testing.

The article also discussed how highly crystalline polymers are generally brittle at room temperature due to their strong molecular bonds. If a polymer is loaded with a high strain-rate, it will exhibit brittle properties because the chains will not have sufficient time to realign themselves as they can with good mobility under a continuous force. In other words, if a polymer is loaded slowly, the material will deform more easily because chain realignment can occur (Brown et al., 2009). This further supports the importance of dynamic compressive testing as a means to understand the polycarbonate samples because the results for this experiment could have been unique to the rate at which the load was applied. It is possible that the same samples under quasi-static testing could have indicated a different stress response upon additional UV degradation. Figure 21 presents a graph borrowed from Brown's article. In this figure, a stress-stain plot is presented with three curves representing different polymer states. The figure clearly shows a higher stress response for brittle polymers tested to failure as compared to plastic polymers tested to failure.

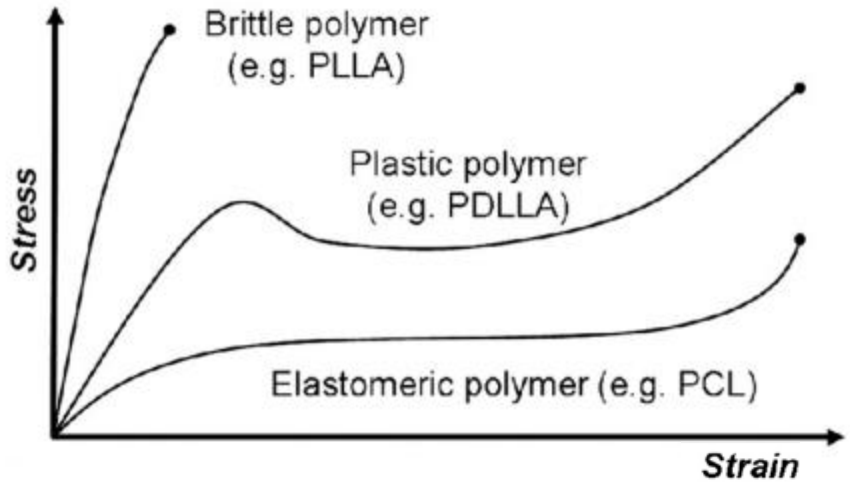

Figure 21. Stress/strain relationships for brittle, plastic, and elastomeric polymers.(Brown et al., 2009)

CONCLUSION

To conclude, this experiment was performed with the objective of understanding the effects of UV degradation on polycarbonate plastics. This was performed by placing rods of polycarbonate in a QUV accelerated weathering machine under a fluorescent bulb for 375 hours, 750 hours, and 1500 hours. These rods, in addition to a control group, were then tested by means of dynamic compression using a Split-Hopkinson Pressure Bar. The test was run with an average strain rate of 1600/s. The voltage change recorded from strain gauges attached on the incident and transmission rods allowed for the creation of stress vs strain plots to compare the different samples.

The results showed an excellent amount of precision between the samples in each group. The available results indicated that the plateau strength was very similar for the control, 375 hour, and 750 hour sample group and then increased for the 1500 hour group to 169.03MPa which was a 35.51% increase in comparison to the 124.73MPa average plateau stress for the control group. The energy density was also calculated for each time span group at sample strain of 25% and the same trend was noticed. The control, 375, and 750 hour groups had similar energy densities while the 1500 hour samples had an energy density of 37.54 kJ/m^3 which was 32.64% more than the control group energy density value of 28.30 kJ/m^3.

This response was contrary to initial thoughts on the effects and behavior of UV exposure on the polycarbonate which indicated that exposure would weaken the samples. However, after further research the results can be explained very simply. The exposure to

UV light from the fluorescent bulbs began to cause embrittlement in the structure of the plastics. This embrittlement resulted in an initial increase in strength. The test methods used in this experiment did not test the samples to failure to accurately analyze the toughness to understand which properties of the plastics were compromised in the accelerated weathering process. This explanation remains conjecture without significant data to understand the failure behavior of the samples. The scope of the project was able to analyze polycarbonate under UV exposure for 1500 hours or less in dynamic compression. This was successfully completed during this experiment.

In further research, testing the samples to failure should be of primary concern to truly understand the dynamic response of polycarbonate subjected to UV weathering and any compromises that may exist due to the increase in strength found in this experiment. This could be done by changing the testing method to a tensile testing system. This test would allow for an analysis of the dynamic response but it would not be compressive as was studied in this experiment.

Compression testing to failure could be accomplished by increasing the duration of the experiment. The duration of the stress pulse during the experiment is directly related to the length of the striker rod (*ASME*), so increasing the striker rod length in the experimental setup could allow for a longer test and more encompassing data. This could allow the samples to be tested to failure to be able to truly understand the dynamic compression and any compromises that may exist due to the increase in strength.

Other changes in the experiment could be incorporated to improve the testing results. For example, research has been done that indicates that mounting strain gauges

directly to the specimen could result in a more accurate determination of strain (Li & Lambros, 1999). This would be interesting to experiment with to see if the data differs.

It would be interesting to test polycarbonate plastics without the presence of additives to reduce the effects of UV exposure. This would allow for a more wholistic view of polycarbonate and its reaction to UV without having to consider the properties in the additives.

The experiment could also be expanded by performing further research to analyze the samples and their effects to longer amounts of exposure beyond the scope of this project. Longer amounts of exposure could introduce new trends not available in this data. It is possible that this experiment did not use sufficient exposure times to introduce enough damage to the samples.

Other weathering techniques or bulbs could also be utilized to simulate the desired external weathering parameters. Weathering involves many components, so it could be beneficial to explore different parameters to attempt to replicate natural weathering. Utilizing several of these changes in further research could allow for a natural continuation of the understanding of polycarbonate plastics subjected to UV degradation and tested under dynamic compressive loading conditions. This could be beneficial in providing an opportunity to further understand a material that is becoming increasingly useful in modern manufacturing and design.

BIBLIOGRAPHY

British Plastics Federation. (n.d.). *Polycarbonate (PC)*. https://www.bpf.co.uk/plastipedia/polymers/Polycarbonate.aspx

Brown, D. A., Lee, E. W., Loh, C. T., & Kee, S. T. (2009). A new wave in treatment of vascular occlusive disease: Biodegradable stents—clinical experience and scientific principles. *Journal of Vascular and Interventional Radiology*, *20*(3), 315–324. https://doi.org/10.1016/j.jvir.2008.11.007

Federoff et. Al "A physically motivated element deletion criterion for the concrete damage plasticity model" 2017 Conference: SMiRT-24, At Busan, Korea

Grand View Research. (2021). *Polycarbonate market size, Share & Trends report, 2030*. Polycarbonate Market Size, Share & Trends Report, 2030. https://www.grandviewresearch.com/industry-analysis/polycarbonate-market

Ivy Turner, "High Strain-Rate Sensitivity and Energy Absorption of DuroProtect, a Fiber-Reinforced Ballistics Composite", ECTC Conference 2019

Li, Z., & Lambros, J. (1999). Determination of the dynamic response of brittle composites by the use of the Split Hopkinson Pressure Bar. *Composites Science*

and Technology, 59(7), 1097–1107. https://doi.org/10.1016/s0266-3538(98)00152-3

Lotti Tajouri Associate Professor, Matthew Olsen Assistant researcher, Rashed Alghafri Honorary Adjunct Associate Professor, & Simon McKirdy, Professor of Biosecurity. (2023, October 19). *Tempted to buy a UV light disinfection gadget? some can be dangerous – here's what you need to know*. The Conversation. https://theconversation.com/tempted-to-buy-a-uv-light-disinfection-gadget-some-can-be-dangerous-heres-what-you-need-to-know-194065

Mantena, Raju, "ME 416 Structures and Dynamics Laboratory", University of Mississippi, Printing Services, 2023

McKeen, L. W. (2013). *The effect of UV light and weather on plastics and elastomers* (Third). William Andrew.

National Aeronautics Space Administration, Science Mission Directorate. (2010). *Ultraviolet waves*. NASA. https://science.nasa.gov/ems/10_ultravioletwaves/

Shokrieh, M. M., & Bayat, A. (2007). Effects of ultraviolet radiation on mechanical properties of glass/polyester composites. *Journal of Composite Materials*, *41*(20), 2443–2455. https://doi.org/10.1177/0021998307075441

Southwest Research Institute. (n.d.). *Split-Hopkinson Pressure Bar Apparatus*. San Antonio, Texas. Retrieved February 16, 2024, from https://www.asme.org/about-asme/engineering-history/landmarks/242-split-hopkinson-pressure-bar-

apparatushttps://www.asme.org/about-asme/engineering-history/landmarks/242-split-hopkinson-pressure-bar-apparatus.

Stoddard, D., Ukyam, S. B., Tisserat, B., Turner, I., Baird, R., Serafin, S., Torrado, J., Chaudhary, B., Piazza, A., Tudor, M., & Rajendran, A. M. (2020). High strain-rate dynamic compressive behavior and energy absorption of distiller's dried grains and soluble composites with paulownia and pine wood using a split Hopkinson pressure bar technique. *BioResources*, *15*(4), 9444–9461. https://doi.org/10.15376/biores.15.4.9444-9461

P. Raju Mantena, (2012). "Strain Gauging/stress Analysis/Digital Image Correlation." Engr 314 MATERIAL SCIENCE LABORATORY. Department of Mechanical Engineering.TheUniversity of Mississippi

Wu, X. J., & Gorham, D. A. (1997). Stress equilibrium in the Split Hopkinson Pressure Bar Test. *Le Journal de Physique IV*, *07*(C3). https://doi.org/10.1051/jp4:1997318

Yousif, E., & Haddad, R. (2013). Photodegradation and photostabilization of polymers, especially polystyrene: Review. *SpringerPlus*, *2*(1). https://doi.org/10.1186/2193-1801-2-398

Zhang, H. (Ed.). (2011). The basic properties of building materials. *Building Materials in Civil Engineering*, 7–423. https://doi.org/10.1533/9781845699567.7